Impact of the Doping Method on Conductivity and Thermopower in Semiconducting Polythiophenes

*Anne M. Glaudell, Justin E. Cochran, Shrayesh N. Patel, and Michael L. Chabinyc**

The development of organic semiconductors for use in thermoelectrics requires the optimization of both their thermopower and electrical conductivity. Here two fundamentally different doping mechanisms are used to investigate the thermoelectric properties of known high hole mobility polymers: poly 3-hexylthiophene (P3HT), poly(2,5-bis(3-tetradecylthiophen-2-yl)thieno[3,2-b]thiophene) (PBTTT-C_{14}), and poly(2,5-bis(thiphen-2-yl)-(3,7-diheptadecantyltetrathienoacene)) (P2TDC$_{17}$-FT4). The small molecule tetrafluorotetracyanoquinodimethane (F_4TCNQ) is known to effectively dope these polymers, and the thermoelectric properties are studied as a function of the ratio of dopant to polymer repeat unit. Higher electrical conductivity and values of the thermoelectric power factor are achieved by doping with vapor-deposited fluoroalkyl trichlorosilanes. The combination of these data reveals a striking relationship between thermopower and conductivity in thiophene-based polymers over a large range of electrical conductivity that is independent of the means of electrical doping. This relationship is not predicted by commonly used transport models for semiconducting polymers and is demonstrated to hold for other semiconducting polymers as well.

1. Introduction

Organic electronic materials have found recent success in applications from solar cells to transistors and displays.[1–3] Semiconducting polymers can be deposited on flexible substrates, and processed at room temperature, thus reducing the energy needed to manufacture devices compared to inorganic materials. These features also lend themselves to alternative manufacturing techniques for electronics: inkjet printing, roll-to-roll processing, and screen printing.[4] Despite the recent progress in applications, charge transport is still not well understood in semiconducting polymers. An improved understanding of transport will lead to the ability to design new materials and open new applications for organic materials.

A. M. Glaudell, Dr. S. N. Patel, Prof. M. L. Chabinyc
Materials Department and Materials Research Laboratory
University of California Santa Barbara
Santa Barbara, CA 93106–5050, USA
E-mail: mchabinyc@engineering.ucsb.edu
Dr. J. E. Cochran
Department of Chemistry and Biochemistry
University of California Santa Barbara
Santa Barbara, CA 93106–9510, USA

DOI: 10.1002/aenm.201401072

A critical need for organic semiconductors is the ability to control their electrical conductivity. In addition to measurements of conductivity, the thermopower (Seebeck coefficient) offers a unique view into transport; it provides direct access to the entropy per carrier.[5,6] Thermopower measurements combined with conductivity measurements can offer a clearer picture of transport mechanisms than what is offered by electrical measurements alone.

Unlike conventional inorganic semiconductors, doping of organic materials usually requires introduction of a large molecular species that may disrupt the molecular organization. Here, we examine how doping using two approaches leads to a surprising trend in the thermopower as a function of electrical conductivity for a series of organic semiconducting polymers. This relationship is compared to predictions from several transport models commonly applied to organic semiconductors. The empirical trend provides guidance by which to determine improvements in the thermoelectric performance of organic semiconductors. One may use this trend to see if new materials have thermoelectric properties consistent with those previously studied. For instance, if a new material had a lower electrical conductivity than expected for the measured thermopower, this may be indicative of morphology-limited conductivity.

Only recently have organic electronic materials been seriously considered for thermoelectrics and they could enable fabrication of flexible thermal energy scavengers and heating/cooling devices.[7,8] Traditional thermoelectric modules consist of rigid and brittle materials rendering them relatively fragile limiting their application in some cases. The ability to process organic electronic materials on a flexible substrate opens up the possibility of conformal device geometries for niche applications such as comfortable wearables and portable/roll out thermoelectric generators or coolers. The challenge for organic thermoelectric materials lies in enhancing and controlling the electronic properties, as well as adapting device morphology for solution-processable semiconducting materials.

The power conversion efficiency of a thermoelectric material is related to the thermoelectric figure of merit $ZT = \left(\alpha^2\sigma/\kappa\right)/T$, where α is the Seebeck coefficient, σ is electrical conductivity, κ is thermal conductivity, and T is temperature. The sign of the thermopower α indicates the type of the majority carrier. The three parameters α, σ and κ are counter-indicated and

interrelated as a function of carrier concentration, resulting in a maximum ZT at an intermediate carrier concentration. The thermal conductivity κ is the sum of two components: κ_L from the lattice, and κ_E, the electronic component from the charge carriers. The main challenge for the development of inorganic thermoelectric materials is lowering the thermal conductivity while maintaining their electrical properties. Polymers on the other hand, have a low lattice thermal conductivity due to their disordered morphology. Because the electronic component of the thermal conductivity is unlikely to contribute until very high electrical conductivities (>1000 S cm^{-1}), the main emphasis currently is to understand how to optimize their electrical properties, i.e., the power factor $PF = \alpha^2\sigma$.

The thermopower α is directly related to the electronic density of states (DOS) of a material. Fritzche derived a general expression for thermopower in relation to the conductivity DOS $\sigma(E)$:[5]

$$\alpha = \frac{k_B}{e}\int \frac{E - E_F}{k_B T}\frac{\sigma(E)}{\sigma}\mathrm{d}E \quad (1)$$

where E_F is the Fermi energy, σ is the absolute conductivity, and k_B/e is a natural unit of thermopower equal to 86.17 μV K^{-1}. The conductivity density of states $\sigma(E)$ can be represented in the following way, given $\sigma = e\mu n$, where μ is carrier mobility, and n is carrier concentration:[5]

$$\sigma(e) = e\mu(E)g(E)f(E)\left[1 - f(E)\right] \quad (2)$$

Here, $\mu(E)$ is the mobility as a function of energy, $g(E)$ is the density of states, and $f(E)$ is the Fermi distribution. Deriving a relation of thermopower as a function of conductivity for various transport mechanisms is non-trivial, and many proposed relations of $\alpha(\sigma)$ are not derived from models, but fit the data and qualitatively related to transport.[9–11] The reason being that while the DOS has been studied for many materials in diodes and thin film transistors, it is unclear how parameters in Equation (1) change as a function of doping, especially in the case of molecular doping, which may significantly change molecular ordering. Semiconducting polymers complicate the determination of a relation due to their heterogeneous morphology because they are composed of both ordered and disordered regions that may exhibit different fundamental transport mechanisms.

Studies of the thermoelectric properties of foundational semiconducting polymers including polyacetylene, polyaniline, and polypyrrole have been made in the context of fundamental transport mechanisms. Much of this work addressed aligned or highly anisotropic polymers doped with ions such as iodine, enabling metallic levels of conductivity. Although the thermoelectric figure of merit ZT and power factor PF were often not calculated or addressed, these materials turn out to have relatively high power factors, up to 1.49 mW m^{-1} K^{-2} for iodine-doped stretch-aligned polyacetylene at 6.1×10^4 S cm^{-1}.[12] However, this class of polymers is a poor choice for applications. The metallic levels of conductivity are in general temporary, reliant upon an overpressure or constant presence of the dopant vapor. The high anisotropy due to alignment of these polymers is shown to significantly increase the thermal conductivity of the material in the direction of transport, possibly negating the advantage of polymers in the first place and limiting ZT.[13] More recently, poly(3,4-ethylenedioxythiphene) (PEDOT) derivatives dominate the research on organic and hybrid thermoelectric materials.[14] These are widely used as an environmentally stable transparent conducting electrode in organic photovoltaic devices, and there are many well-documented methods to vary the conductivity of the film.

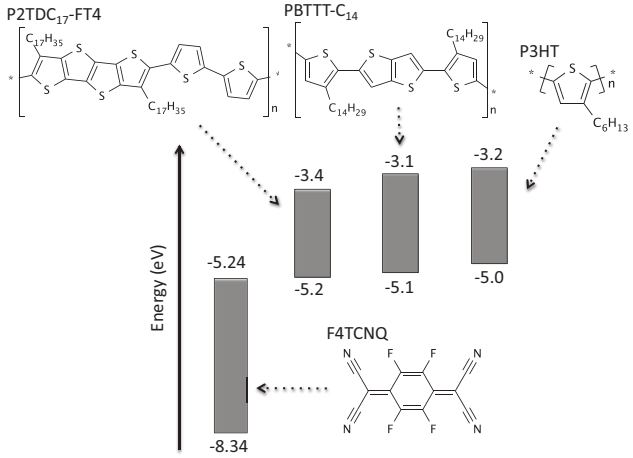

Figure 1. Molecular structure and highest occupied molecular orbital (HOMO)/lowest unoccupied molecular orbital (LUMO) levels of polymers P3HT,[24,45,46] PBTTT-C_{14},[22,47] and P2TDC$_{17}$-FT4,[48] in addition to the small molecule F_4TCNQ.[49]

Here, we study the role of the doping method on the electrical conductivity and thermopower of a series of structurally related semiconducting polymers. These materials are all known to have high carrier mobilities in thin film transistors and help to provide a benchmark for understanding the performance of polymers for thermoelectrics. By comparing our work to data from the literature, we find an unusual trend in the PF over a very large range (10^{-5}–10^3 S cm^{-1}) of electrical conductivity, which differs from conventional inorganic thermoelectric materials.

2. Results

There have been few investigations into the effect on thermoelectric properties of various doping mechanisms with a consistent set of polymers.[15] Here, we examine a structurally similar series of polymers known to perform well in thin-film transistors. Three polymers were investigated in this study (shown in **Figure 1**): poly 3-hexylthiophene (P3HT), poly(2,5-bis(3-tetradecylthiophen-2-yl)thieno[3,2-b]thiophene) (PBTTT-C_{14}), and poly(2,5-bis(thiphen-2-yl)-(3,7-diheptadecantyltetrathienoacene)) (P2TDC$_{17}$-FT4). These polymers have known high hole-mobility and possess crystalline, ordered regions as well as amorphous, disordered regions.[16] P3HT and PBTTT-C_{14} have similar trap-free mobilities (≈1 to 10 cm^2 V^{-1} s^{-1});[17–20] by extension, we also chose P2TDC$_{17}$-FT4.[21] Experimentally measured carrier mobilities in these polymers differ due to microstructural ordering and processing.[16,21–23]

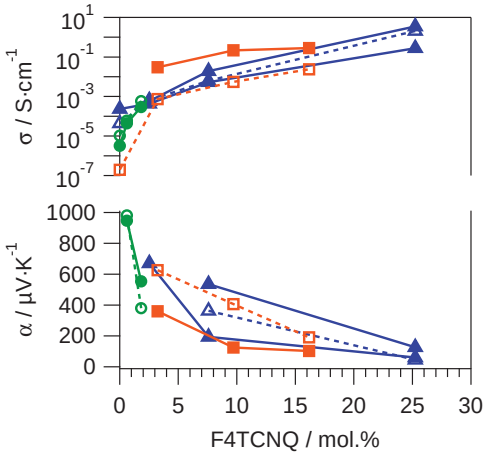

Figure 2. Conductivity (top) and thermopower (bottom) as a function of molar ratio of F_4TCNQ to polymer repeat unit (mol%) for P3HT (●), PBTTT-C_{14} (▲), and P2TDC$_{17}$-FT4 (■). Samples are either as cast (open symbols, dashed lines), or annealed at 150°C for 10 minutes (solid symbols and lines). The two solid traces for annealed PBTTT are from films made from different solutions to show the reproducibility of the measurement.

The polymers were doped in two separate ways: in solution with the small molecule tetrafluorotetracyanoquinodimethane (F_4TCNQ), and via vapor deposition of the alkyl silane (tridecafluoro-1,1,2,2,-tetrahydrooctyl)-trichlorosilane (FTS) onto the surface of the polymer thin film. F_4TCNQ is known to effectively hole-dope these polymers via charge transfer.[24,25] FTS has also been shown to dramatically enhance conductivity in PBTTT-C_{14} and P3HT, far beyond 10 S cm^{-1}.[26] There is evidence that F_4TCNQ inserts itself into the ordered regions of the polymer, disrupting the molecular packing of the neat material.[16,24,25,27] By contrast, it is thought that the vapor-deposited FTS forms a self-assembled monolayer, or at least a thin film, on the surface of the semiconducting film leading to doping stabilized by a surface dipole.[26] The precise mechanism of doping is still uncertain. Grazing-incidence wide angle X-ray scattering (GIWAX) results on FTS-doped PBTTT-C_{14} films indicate that the FTS causes a small disruption of the crystallite size, but does not incorporate into the ordered crystalline domains as observed with F_4TCNQ doping (see Supporting Information and Figure S7 therein).

For polymers doped with F_4TCNQ, a wide range of conductivities was obtained by varying the weight ratio of dopant to polymer in solution. For all three polymers, conductivity increases by increasing the weight ratio of dopant to polymer in solution. A 10-fold increase in dopant concentration from 2.5 mol% (1 wt%) to 25 mol% (10 wt%) for PBTTT-C_{14} resulted in an increase of conductivity by nearly four orders of magnitude, from 6.37×10^{-4} S cm^{-1} to 2.08 S cm^{-1}. P3HT and P2TDC$_{17}$-FT4 followed similar trends, with the results summarized in **Figure 2**. This finding agrees with previous studies of F_4TCNQ-doped polythiophenes.[24]

The thermal stability of the F_4TCNQ-doped films can be seen in electrical conductivity measurements of as-cast and annealed thin films of each doping level and polymer (Figure 2). For P3HT and PBTTT-C_{14} at the doping levels reported, there were only small changes between samples measured as cast versus annealed at 150 °C for 10 min under dry nitrogen, and similarly small differences from solution-to-solution. F_4TCNQ was less compatible as a dopant in P2TDC$_{17}$-FT4, as the film conductivity values were not stable to annealing, even at lower annealing temperatures. As cast films exhibited variation in conductivity across different solutions, indicating that F_4TCNQ is a less stable dopant in P2TDC$_{17}$-FT4 solution than in P3HT or PBTTT-C_{14} solutions. For more details refer to the Supporting Information (Figure S10). Further processing optimization may be necessary for future studies using this polymer/dopant system.

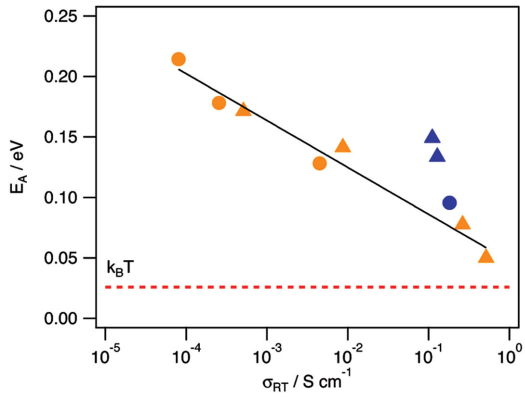

Figure 3. Activation energies as a function of room-temperature conductivity σ_{RT} for F_4TCNQ-doped (yellow) and FTS-doped (blue) P3HT (●) and PBTTT-C_{14} (▲). The solid line is a log fit to the F_4TCNQ-doped polymer data. Activation energies were determined by the slope of an Arrhenius plot of temperature dependent conductivity.

An Arrhenius plot of temperature-dependent electrical conductivity measurements confirm that the conductivity is thermally activated below 270 K for the F_4TCNQ-doped polymers (Supporting Information Figure S8), and below 300 K for FTS-doped polymers (Supporting Information Figure S9), with activation energies determined by the Arrhenius expression for activated transport: $\sigma = \sigma_0 \exp(E_A / k_B T)$. Furthermore, a plot of the calculated activation energies E_A shows that E_A is proportional to the absolute value of $\ln(\sigma_{RT})$, where σ_{RT} is the conductivity at room temperature (300 K) (**Figure 3**). The parameter σ_0 slightly increased with increasing conductivity, with no clear trend between samples. **Table 1** summarizes the Arrhenius fitted parameters for each sample measured.

Thermopower was measured in identically and simultaneously processed samples as conductivity to maintain accurate comparison between conductivity and thermopower. For P3HT, PBTTT-C_{14}, and P2TDC$_{17}$-FT4 doped with F_4TCNQ, the thermopower decreased with increasing dopant ratio, as expected for semiconductors. Thermopower showed similar stability as conductivity for as-cast and annealed films, with little change upon annealing for P3HT and PBTTT-C_{14}, and larger changes for P2TDC$_{17}$-FT4 (Figure 2).

For the polymer thin films doped with FTS, a wide range of conductivities was obtained by partially doping films, or by exposing fully doped films to ambient atmosphere, humidity and illumination, for varying amounts of time, thereby de-doping the film over time (see Supporting Information for more details). Kept under inert conditions (nitrogen environment), the films maintain the conductivity resulting

Table 1. Activation energy and Arrhenius parameters extracted from temperature-dependent conductivity measurements.

Polymer	mol% F_4TCNQ	σ_{RT} [S cm^{-1}]	E_A [meV]	σ_0 [S cm^{-1}]
PBTTT-C_{14}	2.5	5.1×10^{-4}	170	0.40
	7.6	8.7×10^{-3}	140	3.3
	12	2.6×10^{-1}	78	11
	25	5.2×10^{-1}	50	8.2
P3HT	0.60	8.1×10^{-5}	210	0.31
	1.8	2.5×10^{-4}	180	0.25
	3.0	4.5×10^{-3}	130	0.63
PBTTT-C_{14}	FTS	1.3×10^{-1}	130	23
	FTS	1.1×10^{-1}	150	34
P3HT	FTS	1.8×10^{-1}	100	7.7

from the processing method, i.e., returning de-doped films to inert conditions halts the de-doping process. The electrical conductivities reached as high as 27.7 S cm^{-1} for P3HT and 604 S cm^{-1} for PBTTT-C_{14}. These values are nearly as high as those reported elsewhere for FTS doping (≈50 S cm^{-1} for P3HT, ≈1100 S cm^{-1} for PBTTT-C_{14}).[26] We attribute this difference to brief exposure to atmosphere, which is unavoidable in the current experimental setup. The thermopower is also inversely correlated with doping, indicated by in inverse correlation with conductivity discussed later. There seems to be no difference in performance for intermediate-doped versus de-doped films, as there is no hysteresis evident in the thermopower vs conductivity curve (**Figure 4**). The thermoelectric parameters of the highest-performing compositions are summarized in **Table 2**.

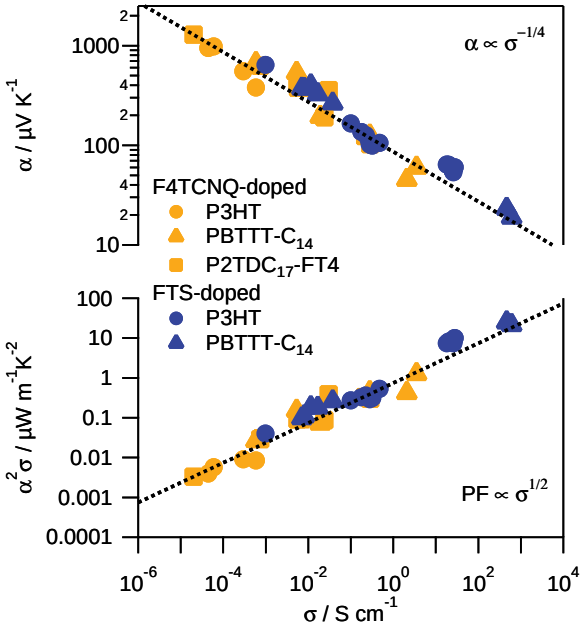

Figure 4. Thermopower (top) and power factor (bottom) as a function of electrical conductivity for F4TCNQ-doped polymers (yellow) P3HT (●), PBTTT-C_{14} (▲), and P2TDC$_{17}$-FT4 (■) and FTS-doped polymers (blue) P3HT (●), and PBTTT-C_{14} (▲). The dashed lines indicate an empirical fit of α proportional to $\sigma^{-1/4}$ and PF proportional to $\sigma^{1/2}$.

Table 2. Conductivity, thermopower, and calculated power factor for the highest-performing films measured.

Film/dopant	σ_{RT}[a)] [S cm^{-1}]	α[b)] [μW K^{-1}]	PF [μW m^{-1}K^{-2}]
PBTTT-C_{14} /F_4TCNQ (25 mol%)	3.51 ± 0.05	60 ± 9	1.3 ± 0.4
P3HT/FTS	27.7 ± 0.1	60 ± 9	10 ± 3
PBTTT-C_{14}/FTS	604.0 ± 0.7	19 ± 3	22 ± 7
PBTTT-C_{14}/FTS	466.0 ± 0.1	23 ± 4	25 ± 8

[a)]Conductivity error calculated as sample standard deviation over at least 3 measurements over 1 or more samples; [b)]Thermopower error is given by the standard error of the thermopower measurement system at 15%.

3. Discussion

The relationship between the thermopower and electrical conductivity in a semiconductor can best be understood if the carrier concentration is known. However, the carrier concentration cannot be measured directly in polymer films via traditional measurements over a wide range of conductivities due to energetic disorder.[10,28] Poorly conducting films have carrier mobilities that are too low for the Hall effect measurement to be useful and at high conductivity the interpretation of the Hall coefficient is difficult in disordered materials.[28] While electronic spin resonance (ESR) can be used at low carrier concentration to measure spin concentrations, the more highly conducting films exhibit both polarons and spinless bipolarons, the latter of which are silent in ESR.[29,30] It is also unclear if the molar ratio of the dopant to the polymer is representative of the free carrier concentration. As a consequence, we compare the thermopower α and power factor PF to the electrical conductivity σ instead of to the carrier concentration p or nominal molar percent doping. This method has proven to be successful for providing an understanding of the behavior of inorganic semiconductors, although it is not as widely applied for organic materials.[31]

A clear trend emerges when comparing thermoelectric properties of all three polymers across both doping schemes Figure 4. The thermopower curve is fit to an empirical power law:

$$\alpha = \frac{k_B}{e}\left(\frac{\sigma}{\sigma_\alpha}\right)^{-1/4} \quad (3)$$

Here, k_B/e is the Boltzmann constant divided by unit charge, or the natural unit of thermopower 86.17 μV K^{-1}. The parameter σ_α is an unknown conductivity constant independent of carrier concentration in the range covered, and fit to approximately 1 S cm^{-1}. It is unclear as to what physical significance σ_α carries from this empirical fit. An additive constant to Equation (3) does not change the value of σ_α dramatically. On a double logarithmic plot, adjusting σ_α shifts the thermopower trend line up or down. Increasing σ_α causes the fit to overestimate the thermopower with the absolute effect largest in the lower conductivity region; decreasing σ_α underestimates the thermopower similarly. The power factor consequently then has a square root dependence on conductivity, $PF \propto \sigma^{1/2}$. We have compiled

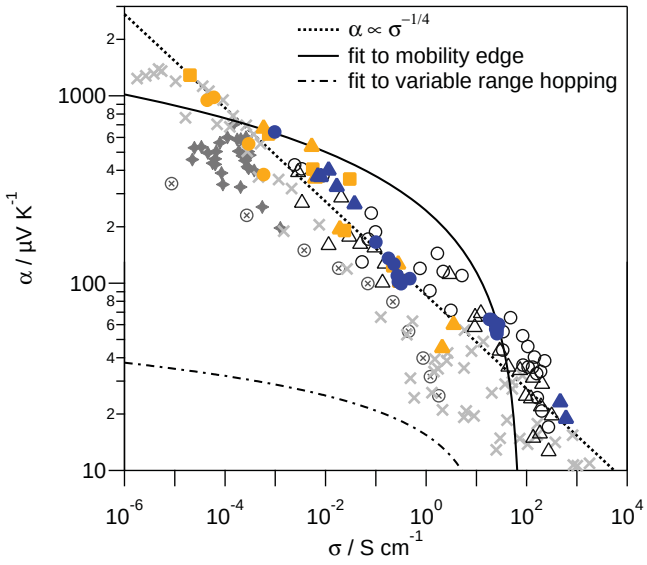

Figure 5. Compilation of thermopower vs conductivity data from this study: F_4TCNQ-doped polymers (yellow) P3HT (●), PBTTT-C_{14} (▲), and P2TDC$_{17}$-FT4 (■) and FTS-doped polymers (blue) P3HT (●), and PBTTT-C_{14} (▲), and select literature data: P3HT doped with PF_6^-(⊗),[32] P3HT:P3HHT doped with F_4TCNQ (♦),[50] P3HT (○) and PBTTT (Δ) doped with $TFSI^-$,[15] and polyacetylene with various dopants (×) (compiled from ref. [10]. The dotted line indicates the empirical fit; the solid line indicates a mobility edge model using the activation energies measured for F_4TCNQ-doped P3HT and PBTTT-C_{14}.

thermoelectric data from the literature and show a comparison of those to the data reported here in **Figure 5**; this further demonstrates this empirical relationship. Previous studies of optimization of the thermoelectric properties of P3HT doped with F_4TCNQ[50] and PF_6^- anions[32] also appear to follow the trend line, although the range of electrical conductivity was limited. Data from a recent study of PBTTT, P3HT, and other polythiophenes doped with ferric salt with bis(trifluoromethane)sulfonimide (TFSI) also follows the empirical trend over a large conductivity range.[15]

It is startling that this trend fits over 9 orders of magnitude of conductivity, for both doping mechanisms, and across semiconducting polymers. It can be safely assumed that the transport mechanism at the lowest end of the conductivities measured is much different than at the highest end of conductivities measured, even if only considering the F_4TCNQ-doped films. A measure of the activation energies of the F_4TCNQ-doped polymers shows that at the highest doping loads, the activation energy approaches k_BT, near which the transport mechanism is expected to change dramatically[6] (Figure 3). Additionally, the two doping mechanisms are fundamentally different at a microstructural level. As stated earlier, the F_4TCNQ intercalates in between the ordered polymer chains and may or may not be present in the disordered regions. Adding more F_4TCNQ from dilute to saturation concentrations changes the morphology of the film. The FTS films are doped to saturation, and de-doped with humidity and illumination, with no evidence that the FTS is leaving the surface of the film.[26] The morphology of the doped and de-doped films is assumed to be identical within the active region. Partially doping the films with incomplete coverage of FTS is indistinguishable from a de-doped film when comparing measured conductivity and Seebeck coefficient.

Previous analyses of thermopower as a function of conductivity in other studies of semiconducting polymers have found one of two empirical relations: either $\alpha \propto \ln\sigma$ or the same $\alpha \propto \sigma^{-1/4}$ exhibited by our systems. A few models for charge transport in polymers do yield $\alpha \propto \ln\sigma$. A $\ln\sigma$ dependence of thermopower emerges from bipolaron hopping within the Holstein-Hubbard model for molecular crystals.[32] This model results in $\alpha \propto -\ln\sqrt{c}$ and $\sigma \propto \sqrt{c}$, where c is the concentration of charge-carrying polarons and bipolarons, thus $\alpha \propto \ln\sigma$. This analysis was suggested to qualitatively explain the $\ln\sigma$ dependence found for PF_6^- doped P3HT by Xuan et al. over a wide range of conductivities ≈1 S cm^{-1} down to ≈10^{-5} S cm^{-1} (data included in Figure 5).[32] However, experimental data were shown to have a much stronger doping dependence of thermopower and conductivity than what is predicted by this model.[32]

Analysis of stretch-aligned polyacetylene, polypyrrole, and polyaniline by Mateeva et al. shows the following $\ln\sigma$ relation:[11]

$$\alpha = -\frac{k_B}{e}\frac{1}{\beta}\ln\left(\frac{\sigma}{\sigma_{max}}\right) \quad (4)$$

It was found that $\beta \gg 1$ and is dependent on the chemical nature of the dopant, with no universal trend for different dopants across various polymers. Additionally, different values of β and σ_{max} were found depending on whether properties were measured parallel or perpendicular to aligned films. This relationship can also be derived from statistical mechanics, valid for the light doping limit, for a material with only one carrier type, and a material that exhibits a σ_{max} such that $\sigma = \sigma_{max}c(1-c)$.[11] This trend does not exceed the thermopowers measured in this study, and power factor flattens out upon increasing dopant concentration. If $\beta = 1$, we are left with the Mott-Heike formula for thermopower in semiconductors: $\alpha = (k_B/q)\ln(c/(1-c))$.[11,32] This model has been successful in describing transport in inorganic semiconductors including Bi_2Te_3, but is inappropriate for polymers due to disorder.[31,32]

A 2001 review by Kaiser noted a $\alpha \propto \sigma^{-1/4}$ dependence of thermopower on conductivity for a multi-source compilation of polyacetylene data over a similarly wide range of conductivities as this study (Figure 5).[10,33–42] These data were qualitatively related to the variable range hopping model, which describes thermopower as the following:

$$\alpha = -\frac{k_B^2}{e}(T_0T)^{1/2}\left.\frac{d\ln N}{dE}\right|_{E_F} \quad (5)$$

The variable T_0 is found via the temperature dependent Mott relation for conductivity, with $\gamma = 1/3$ chosen in Kaiser's analysis: $\sigma = \sigma_0\exp\left[-(T_0/T)^\gamma\right]$.[6] It was found that the thermopower did track to $T_0^{1/2}$, as expected from Equation (5), and $(d\ln N/dE)$ at the Fermi energy is equal to about 2 eV^{-1}.[33]

The mobility edge model is also often used to describe transport of disordered polymer systems.[16,23] The mobility-edge model for thermopower gives the following temperature-dependent relation for hole transport:[5,6,16]

$$\alpha = \frac{k_B}{e}\left(\frac{E_F - E_V}{k_B T}\right) + A \quad (6)$$

Here, A is dimensionless and greater than 1 and is related to the weighted conductivity density of states, E_F is the Fermi energy, and E_V is the valence energy.[5,6] The activation energy E_A, while not equal to $E_F - E_V$, is correlated to this difference and is used as an estimate, although the activation energy for the thermopower is not necessarily the same as for the electrical conductivity.[43] The activation energy E_A measured for the F_4TCNQ-doped polymers shows $E_A \propto \ln\sigma$, as indicated by the trendline in Figure 3. If we apply the dependence of E_A on conductivity, we find that $\alpha \ln \sigma$ in the mobility edge model:

$$\alpha = \frac{k_B}{e}\left(\frac{B\ln\sigma + C}{k_B T}\right) + A \quad (7)$$

Here, B and C are given by the fit of activation energy to conductivity, shown in Figure 3: $E_A = B\ln\sigma + A$. We see that the mobility edge model (solid line in Figure 5) as used does not fit our data well over many orders of magnitude, regardless of the value chosen for A.

We can also consider variable range hopping in three dimensions, as described in Equation (5). Restricting the parameter $T_0 = E_A / k_B$ to the activation energy relation found experimentally, and assuming that the shape of the density of states at the Fermi level $\left(\mathrm{d}\ln N / \mathrm{d}E\right)_{E=E_F}$ does not vary dramatically with doping, we can see that our data does not strictly fit the VRH hopping model either (long dashed line, Figure 5). The effect of molecular doping on the density of states in semiconducting polymers is not well known, therefore we use the simplest assumption here. We expect this assumption to be reasonable for higher carrier densities, where the Fermi energy is away from the trap states. This fit is displayed for a choice of $\left(\mathrm{d}\ln N / \mathrm{d}E\right)_{E=E_F} = 10\ \mathrm{eV}^{-1}$. Decreasing this parameter moves the trace down, further away from the data.

It is not obvious that the theoretical models should fit the striking trend observed over the whole range of conductivities. The transport mechanism changes dramatically as carrier concentration increases from intrinsic levels to metallic levels. One possible explanation for the trend across this wide range of conductivities is that there is a smooth transition from a model that represents transport well at low carrier concentrations to one that represents carrier concentrations at very high carrier concentrations. Such a fit would also require a consistent DOS for the materials over the wide range of electrical conductivity studied. Surprisingly the same trend is observed for polyacetylene, which has a degenerate ground state, and the thiophene-based materials, which have non-degenerate ground states. Such behavior may indicate a connection between the electronic structure and morphology required to achieve high electrical conductivity, but it is premature to speculate on the necessary physical origin.

It is seen via temperature-dependent conductivity measurements that transport is activated at higher conductivities in the semiconducting polymers. The presence of activated transport is indicative of disorder but may not describe transport in the ordered regions. The temperature-dependence of the thermopower varies more dramatically between transport mechanisms and may reveal more about transport than is limited by conductivity measurements. For example, as the activation energy approaches $k_B T$, the thermopower is linear in temperature.[6] For mobility-edge hopping, it is inversely proportional to temperature (Equation (6). It has been suggested that FTS-doping induces enough charge carriers in P3HT to induce an insulator-to-metal transition, which may be apparent in future studies of the temperature-dependence of the thermopower and the electrical conductivity.

4. Conclusions

We have studied the thermopower of a series of semiconducting polymers using two doping methods. Examination of the power factor over electrical conductivities ranging from $\approx 10^{-5}$ S cm^{-1} to $\approx 10^{3}$ S cm^{-1} shows no obvious maximum in the power factor for these polymers, unlike what is typically observed for inorganic semiconductors. We have not yet seen a maximum power factor where any improvement in the electrical conductivity would be dominated by a loss in thermopower due to an increase in the number of charge carriers. Developing additional doping mechanisms that yield higher conductivities may provide a means to probe the maximum power factor for this class of materials, thus establishing the upper limit of the power factor and thermoelectric figure of merit.

The empirical relationship presented allows a method to determine if new materials exceed the performance of existing materials as thermoelectrics. We also note that to effectively screen materials as good thermoelectric materials, one must measure all the transport properties in the same direction of transport, i.e., in plane or out of plane. In our case, the chain axis of the polymers is known to be along the substrate although it is not oriented over the length scale of the measurements. It is possible that for some materials there is high anisotropy in one, two, or all the transport parameters σ, α, and κ. Device geometries and polymer processing can be chosen to take advantage of the most highly favorable direction for applications.

The surprising correlation of thermopower to electrical conductivity for two very different doping methods and also across polymers raises questions as to the mechanism of charge transport and role of a physical dopant within a polymer blend. This suggests that transport and thermoelectric properties are dominated primarily by the polymer and not by the specific doping mechanism. Temperature-dependent measurements of thermopower of both F_4TCNQ- and FTS-doped polymers are necessary to further explore the mixed transport in these heterogeneous semiconducting polymers.

5. Experimental Section

Samples were prepared by solution casting onto electrically insulating substrates of quartz, glass, or sapphire. Both thick (≈1 μm) and thin (≈50 nm) films were prepared via drop casting in a nitrogen atmosphere or spin-coating in ambient conditions, respectively. All samples were soft-baked at 80 °C in a nitrogen atmosphere for 10 min to remove excess solvent. Annealed samples were baked at 150 °C for 10 min, also under nitrogen.

Gold electrical contacts (45–90 nm thick) were deposited via controlled thermal evaporation through a shadow mask, at an average rate of 1 Å s^{-1}. Two contact geometries were used on simultaneously and identically prepared samples, one each for electrical conductivity and thermopower measurements. Electrical conductivity was measured with a co-linear four-point-probe bar geometry. Thermopower measurement contacts consisted of 1 mm^2 gold pads adjacent to 0.2 mm × 1 mm electrical contact bars, 3 to 5 mm apart (Supporting Information Figure S1). Measurements of thermopower and electrical conductivity were performed under nitrogen, with the exception of temperature-dependent measurements, which were performed under vacuum.

The thermopower was measured via the differential method: a temperature gradient is established across the sample and after a set settling time, five consecutive measurements are taken 1 s apart. The temperature gradient was incremented between approximately ±5 K. Larger stable temperature gradients are possible with the choice of substrate, but the measurement assumes the Seebeck coefficient did not change significantly over $T \pm \Delta T$, so ΔT was kept under 5 K. Each sample was measured multiple times to account for the high percentage of error inherent with thermopower measurements in this system (15%) and in general.[44]

Polymer solutions were made at 5 mg mL^{-1} in a solution of 1:1 chlorobenzene:dichlorobenzene. Solutions were filtered with 0.45 µm PTFE filter at 80 °C. F_4TCNQ-doped samples were made by adding a relative wt% of F_4TCNQ to the polymer solution before casting. FTS-doped samples were doped in a post-processing step by exposing the cast films to FTS vapor in a vacuum oven at 80 °C overnight. Saturation of the doping was assumed to be reached when the films are visibly completely transparent, after which the samples were removed from the chamber. In the short amount of time between the vacuum oven and moving the films to the inert environment, a slight but visible re-coloration of the film indicated slight de-doping, which was unavoidable with the current setup.

Supporting Information

Supporting Information is available from the Wiley Online Library or from the author.

Acknowledgements

The authors gratefully acknowledge support through the AFOSR MURI program under FA9550–12–1–0002. A.E.M received partial support from the ConvEne IGERT Program of the National Science Foundation under NSF-DGE 0801627. J.E.C. received partial support from DOE BES under Award DE- 777SC0005414. This work was partially supported by the MRSEC Program of the National Science Foundation under Award No. DMR 1121053. Use of the Stanford Synchrotron Radiation Lightsource, SLAC National Accelerator Laboratory, is supported by the U.S. Department of Energy, Office of Science, Office of Basic Energy Sciences under Contract No. DE-AC02–76SF00515. The authors wish to thank Prof. Vitaly Podzorov (Rutgers U.) for helpful conversations about doping polymers with FTS vapor.

Received: June 27, 2014
Revised: September 11, 2014
Published online: October 17, 2014

[1] L. Dou, J. You, Z. Hong, Z. Xu, G. Li, R. A. Street, Y. Yang, *Adv. Mater.* **2013**, *25*, 6642.
[2] T. N. Ng, D. E. Schwartz, L. L. Lavery, G. L. Whiting, B. Russo, B. Krusor, J. Veres, P. Bröms, L. Herlogsson, N. Alam, O. Hagel, J. Nilsson, C. Karlsson, *Sci. Rep.* **2012**, *2*, 585.
[3] K. T. Kamtekar, A. P. Monkman, M. R. Bryce, *Adv. Mater.* **2010**, *22*, 572.
[4] R. R. Søndergaard, M. Hösel, F. C. Krebs, *J. Polym. Sci. Part B* **2013**, *51*, 16.
[5] H. Fritzsche, *Solid State Commun.* **1971**, *9*, 1813.
[6] N. F. Mott, E. A. Davis, *Electronic Processes in Non-Crystalline Materials*, Oxford University Press, Oxford **1971**.
[7] O. Bubnova, X. Crispin, *Energy Environ. Sci.* **2012**, *5*, 9345.
[8] O. Bubnova, Z. U. Khan, A. Malti, S. Braun, M. Fahlman, M. Berggren, X. Crispin, *Nat. Mater.* **2011**, *10*, 429.
[9] G. Kim, K. P. Pipe, *Phys. Rev. B* **2012**, *86*, 085208.
[10] A. B. Kaiser, *Rep. Prog. Phys.* **2001**, *64*, 1.
[11] N. Mateeva, H. Niculescu, J. Schlenoff, L. R. Testardi, *J. Appl. Phys.* **1998**, *83*, 3111.
[12] Y. Nogami, H. Kaneko, T. Ishiguro, A. Takahashi, J. Tsukamoto, N. Hosoito, *Solid State Commun.* **1990**, *76*, 583.
[13] P. R. Newman, M. D. Ewbank, C. D. Mauthe, M. R. Winkle, W. D. Smolyncki, *Solid State Commun.* **1981**, *40*, 975.
[14] S. K. Yee, N. E. Coates, A. Majumdar, J. J. Urban, R. A. Segalman, *Phys. Chem. Chem. Phys.* **2013**, *15*, 4024.
[15] Q. Zhang, Y. Sun, W. Xu, D. Zhu, *Macromolecules* **2014**, *47*, 609.
[16] A. Salleo, R. J. Kline, D. M. DeLongchamp, M. L. Chabinyc, *Adv. Mater.* **2010**, *22*, 3812.
[17] M. J. Panzer, C. D. Frisbie, *Adv. Funct. Mater.* **2006**, *16*, 1051.
[18] R. Noriega, J. Rivnay, K. Vandewal, F. P. V. Koch, N. Stingelin, P. Smith, M. F. Toney, A. Salleo, *Nat. Mater.* **2013**, *12*, 1038.
[19] M. J. Lee, D. Gupta, N. Zhao, M. Heeney, I. McCulloch, H. Sirringhaus, *Adv. Funct. Mater.* **2011**, *21*, 932.
[20] J.-F. Chang, J. Clark, N. Zhao, H. Sirringhaus, D. Breiby, J. Andreasen, M. Nielsen, M. Giles, M. Heeney, I. McCulloch, *Phys. Rev. B* **2006**, *74*, 205204.
[21] M. He, J. Li, M. L. Sorensen, F. Zhang, R. R. Hancock, H. H. Fong, V. A. Pozdin, D.-M. Smilgies, G. G. Malliaras, *J. Am. Chem. Soc.* **2009**, *131*, 11930.
[22] I. McCulloch, M. Heeney, C. Bailey, K. Genevicius, I. MacDonald, M. Shkunov, D. Sparrowe, S. Tierney, R. Wagner, W. Zhang, M. L. Chabinyc, R. J. Kline, M. D. McGehee, M. F. Toney, *Nat. Mater.* **2006**, *5*, 328.
[23] M. L. Chabinyc, L. H. Jimison, J. Rivnay, A. Salleo, *MRS Bull.* **2008**, *33*, 683.
[24] P. Pingel, D. Neher, *Phys. Rev. B* **2013**, *87*, 115209.
[25] D. T. Duong, C. Wang, E. Antono, M. F. Toney, A. Salleo, *Org. Electron.* **2013**, *14*, 1330.
[26] C. Y. Kao, B. Lee, L. S. Wielunski, M. Heeney, I. McCulloch, E. Garfunkel, L. C. Feldman, V. Podzorov, *Adv. Funct. Mater.* **2009**, *19*, 1906.
[27] H. Sirringhaus, P. Brown, R. Friend, M. Nielsen, K. Bechgaard, B. Langeveld-Voss, A. Spiering, R. Janssen, E. Meijer, P. Herwig, D. M. de Leeuw, *Nature* **1999**, *401*, 685.
[28] S. Wang, M. Ha, M. Manno, C. Daniel Frisbie, C. Leighton, *Nat. Commun.* **2012**, *3*, 1210.
[29] J. Chen, A. J. Heeger, F. Wudl, *Solid State Commun.* **1986**, *58*, 251.
[30] H. Tanaka, M. Hirate, S. Watanabe, S. Kuroda, *Adv. Mater.* **2014**, *26*, 2376.
[31] D. M. Rowe, G. Min, *J. Mater. Sci. Lett.* **1995**, *14*, 617.
[32] Y. Xuan, X. Liu, S. Desbief, P. Leclère, M. Fahlman, R. Lazzaroni, M. Berggren, J. Cornil, D. Emin, X. Crispin, *Phys. Rev. B* **2010**, *82*, 115454.
[33] A. B. Kaiser, *Phys. Rev. B* **1989**, *40*, 2806.
[34] J. F. Kwak, T. C. Clarke, R. L. Greene, G. B. Street, *Solid State Commun.* **1979**, *31*, 355.
[35] Y. W. Park, A. Denenstein, C. K. Chiang, A. J. Heeger, A. G. MacDiarmid, *Solid State Commun.* **1979**, *29*, 747.

[36] Y.-W. Park, A. J. Heeger, M. A. Druy, A. G. MacDiarmid, *J. Chem. Phys.* **1980**, *73*, 946.
[37] Y. W. Park, W. K. Han, C. H. Choi, H. Shirakawa, *Phys. Rev. B* **1984**, *30*, 5847.
[38] A. J. Epstein, H. Rommelmann, R. Bigelow, H. W. Gibson, D. M. Hoffmann, D. B. Tanner, *Phys. Rev. Lett.* **1983**, *50*, 1866.
[39] M. Galtier, J. M. Gay, A. Montaner, J. L. Ribet, *J. Phys. Colloq.* **1983**, *44*, C3.
[40] M. Przybylski, B. R. Bulka, I. Kulszewicz, A. Proń, *Solid State Commun.* **1983**, *48*, 893.
[41] J. R. Reynolds, J. B. Schlenoff, J. C. W. Chien, *J. Electrochem. Soc.* **1985**, *132*, 1131.
[42] T. E. Jones, T. R. Ogden, W. C. McGinnis, W. F. Butler, D. M. Gottfredson, *J. Chem. Phys.* **1985**, *83*, 2532.
[43] W. Beyer, H. Overhof, *Solid State Commun.* **1979**, *31*, 1.
[44] A. Burkov, in *Thermoelectric Handbook* (Ed: D. Rowe), CRC Press, Boca Raton, FL **2005**.
[45] W. C. Tsoi, S. J. Spencer, L. Yang, A. M. Ballantyne, P. G. Nicholson, A. Turnbull, A. G. Shard, C. E. Murphy, D. D. C. Bradley, J. Nelson, J.-S. Kim, *Macromolecules* **2011**, *44*, 2944.
[46] D. Veldman, S. C. J. Meskers, R. A. J. Janssen, *Adv. Funct. Mater.* **2009**, *19*, 1939.
[47] Q. Sun, K. Park, L. Dai, *J. Phys. Chem. C* **2009**, *113*, 7892.
[48] M. He, J. Li, M. L. Sorensen, F. Zhang, R. R. Hancock, H. H. Fong, V. A. Pozdin, D.-M. Smilgies, G. G. Malliaras, *J. Am. Chem. Soc.* **2009**, *131*, 11930.
[49] W. Gao, A. Kahn, *J. Appl. Phys.* **2003**, *94*, 359.
[50] J. Sun, M.-L. Yeh, B. J. Jung, B. Zhang, J. Feser, A. Majumdar, H. E. Katz, *Macromolecules* **2010**, *43*, 2897.